Antenna Alignment Method for Low Angular Error of 3-axis Tracking System

Jeom Hun Lee*, Young Wan Kim**, Nae Soo Kim* and Ho Jin Lee*

Radio and Broadcasting Technology Lab., ETRI
146-1 Kajong-Dong, Yusong-Gu, Taejon, Korea 305-350

Abstract

This paper describes the antenna alignment method of the tracking antenna system for LEO satellite. The purpose of the antenna alignment is to reduce the angular error due to the structural alignment and the monopulse null point alignment error. The angular error of 3 axis tracking system is the key performance parameter that should be minimized to accurately track satellite movement. The angular error is analyzed via a simulation and boresight measurement. The simulation is done with formulas to be derived from vector concept for 3-axis movement. The formulas of the structural alignment are verified by comparing the formula result with the field measurement. Also, the angular error due to monopulse null shift is obtained via boresight measurement. Based on the analyzed and measured results, the antenna alignment was performed and was verified via tracking test of operating LEO satellite.

Key Word : Antenna alignment, Angular Error, 3-Axis Tracking System

Introduction

After the 3-axis tracking system with tilt axis for the TT&C(Tracking, Telemetry and Command) of satellite is installed at on-site, several factors of the system should be calibrated because of angular error affecting performance of 3-axis tracking system. The sources contributing to the angular error may be classified into four categories, which are servo, structural alignment, mechanical, and RF alignment. The errors due to servo and mechanical can be calibrated at the factory, but the structural and RF alignment that may occur during installation at site should be calibrated prior to operation of antenna. The structural alignment factors are the offsets and scale factors of azimuth, elevation and tilt, north-south offset, and west-east offset. Also, the RF alignment factors are the monopulse null point offset and feed offset.

The method used commonly for the calibration of the structural error is to repeat the test with a reference source such as the boresight antenna, celestial radio stars, or a GEO satellite. This method may be suitable for 2-axis tracking system of azimuth and elevation because the alignment factors of 2-axis system are mostly independent of each other. However, it is very difficult to use this method for the calibration of 3-axis tracking system because the calibration factors of 3-axis system are dependent of each other, which is generated the total performance results in the combination of several factors.

The structural alignment for 3-axis tracking system can be easily resolved via a simulation. The formulas can be obtained by using the vector concept for 3-axis in the presence of the structural alignment error factors. Also, the optimal values of all factors to minimize the angular error are obtained from the simulation with the formula and a reference boresight source.

---

* Senior Researcher
** Principal Researcher
   E-mail : ywk@etri.re.kr, TEL: 042-860-6449, FAX : 042-860-5454

The additional error contributing to the angular error is the monopulse null point error. This error results from the asymmetry allocation among the five horns of antenna or the geometry mismatch between the main and sub-reflector of the antenna

The alignment method of 3-axis monopulse tracking system in this paper is managed via three procedures.

Firstly, to obtain the formulas for the 3-axis operational mechanism from the vector concept for movement of three axes under the assumptions that there are several errors, and to make the monopulse null point alignment model.

Secondly, to verify the structural alignment error and the monopulse null point alignment error of the 3-axis tracking system via the measurement with boresight antenna, and to verify the formula models by comparing the measurement result with simulation result.

Thirdly, to find out the optimal values of all factors from the simulation result to minimize the angular error, and to analyze the alignment result with the angular accuracy concepts. The analyses of these alignment results are done by comparing the result of satellite tracking to be displayed on the ACU(Antenna Control Unit) monitor with the predicted orbit data.

Formula Models

Structural Alignment Formula

The formula is devided into two catogories. One formula is to get the antenna direction angle(azimuth $AZ(\varphi)$ and elevation $EL(\theta)$) for the alignment, which is to find the correction values for the factors contributing to the structural alignment errors. The other formula is to get AZ raw adjusted angle (φ_m) and EL raw adjusted angle (θ_m) to verify the calibration result with the error pattern between the orbit prediction data and the monopulse tracking result[1].

1) Factors of Structural Alignment

The factors contributing to the structural alignment error are north-south tilt, west-east tilt, encoder offsets, and scale factors. These factors are not independent but dependent on the combination of all factors. The definitions of the factors are as follows.

West-East Tilt (θ_{W-E}): It is assumed that the antenna pedestal of the tracking system is installed at the ground planer. However, if the planer has a tilt to west-east direction, it should be corrected after installation.

North-South Tilt (θ_r): For optimal tracking of LEO satellite, the 3-axis tracking system has the 7° tilt toward the north-south direction. This factor should be corrected after installation at on-site because it is really impossible to have exact 7-degree tilt.

Offsets (δ): There are three factors of AZ (δ_{AZ}), EL (δ_{EL}), and tilt offset (δ_{Tilt}), which add the desired angular value to the AZ, EL and tilt position display. These are used to fine-tune the position display. The encoder offsets are added to the actual encoder readings. Thus, a positive offset will increase the apparent antenna position.

Scale Factor (SF): There are three factors of AZ (SF_{AZ}), EL (SF_{EL}), and Tilt Scale factor (SF_{Tilt}), which are used when the ratio between the antenna movement and position encoder input shaft is any value other than 1. The equation for determining the scale factor is as follows:

$$\text{Scale Factor} = \frac{\Delta \text{ Antenna Mechanical Movement}}{\Delta \text{ ACU Position Display}}$$

AZ/EL raw adjusted angle (φ_m, θ_m): This factor is obtained by the simulation or the measurement, and is expressed as the eqn. (20).

2) Formula of AZ(φ), EL(θ)

The antenna direction angle (AZ, EL) of the tracking system always has same direction at 2-axis and 3-axis system for any point on the sky. The vector concept is that the two-axis vector (P'$_{2\text{-axis}}$) of the azimuth and elevation is the same as the three-axis vector (P'$_{3\text{-axis}}$ or P''$_{3\text{-axis}}$) for one point P of free space sky as the eqn. (1) and the Fig. 1[2].

$$P'_{2\text{-axis}} = P'_{3\text{-axis}} = P''_{3\text{-axis}} \tag{1}$$

where the P'$_{3\text{-axis}}$ is the vector not to consider the west-east tilt and the P''$_{3\text{-axis}}$ is the vector to consider it.

Two vectors (P'$_{2\text{-axis}}$ and P'$_{3\text{-axis}}$) with no consideration of the west-east tilt can be obtained from the eqn. (2) and eqn. (3).

$$P'_{2\text{-}axis} = \cos\theta \sin\varphi\, \mathbf{a_x} + \cos\theta \cos\varphi\, \mathbf{a_y} + \sin\theta\, \mathbf{a_z} \tag{2}$$

$$P'_{3\text{-}axis} = \cos\theta_m \sin\varphi_m\, X' + \cos\theta_m \cos\varphi_m\, Y' + \sin\theta_m\, Z' \tag{3}$$
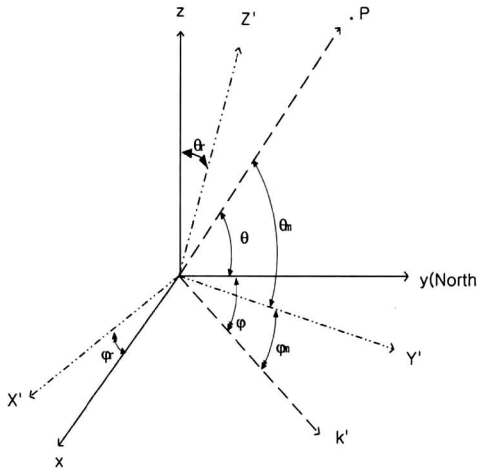

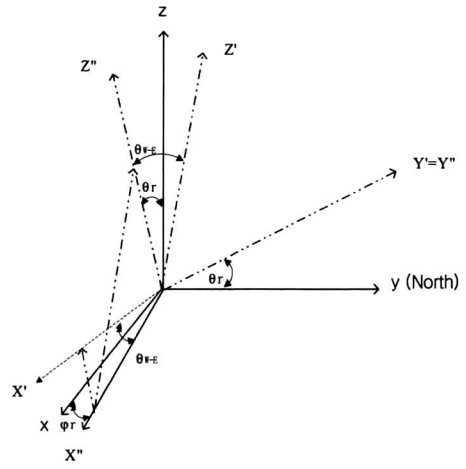Fig. 1. Vectors of 3-axis tracking system without west-east offset ($\theta_{W\text{-}E}$).

Fig. 2. Vectors of 3-axis tracking system with west-east offset ($\theta_{W\text{-}E}$).

The 3-axis vector can be presented as two equations (P'$_{3\text{-axis}}$, P''$_{3\text{-axis}}$) without and with west-east tilt. From the Fig. 1, the 3-axis vector X', Y', and Z' without west-east tilt are obtained as the eqn. (4).

$$X' = \cos\varphi_r \mathbf{a_x} - \sin\varphi_r\, \mathbf{a_y}$$
$$Y' = \cos\theta_r \sin\varphi_r \mathbf{a_x} + \cos\theta_r \cos\varphi_r \mathbf{a_y} + \sin\theta_r \mathbf{a_z}$$
$$Z' = -\sin\theta_r \sin\varphi_r \mathbf{a_x} - \sin\theta_r \cos\varphi_r \mathbf{a_y} + \cos\theta_r \mathbf{a_z} \tag{4}$$

From the Fig. 1 and Fig. 2, the coordinate is rotated to get vector equations for west-east offset. The vector X'', Y'', and Z'' with west-east offset (θ_{W-E}) can be obtained as the eqn. (5).

$$X'' = cos\theta_{W-E}X' - sin\theta_{W-E} Z'$$
$$Y'' = Y' = cos\theta_r \, sin\varphi_r \mathbf{a_x} + cos\theta_r \, cos\varphi_r \mathbf{a_y} + sin\theta_r \mathbf{a_z}$$
$$Z'' = -sin\theta_{W-E}X' + cos\theta_{W-E}Z' \tag{5}$$

Also, the vector P''$_{3-axis}$ is obtained as the eqn. (6).

$$P''_{3-axis} = cos\,\theta_m \, sin\,\varphi_m X'' + cos\,\theta_m cos\,\varphi_m Y'' + sin\,\theta_m Z'' \tag{6}$$

From the eqn. (1) and eqn. (6), the AZ and EL angle as first formula are obtained as eqn. (7) and eqn. (8), respectively.

$$AZ(\varphi) = f(\theta_m, \varphi_m, \theta_{W-E}, \varphi_r, \theta_r) \tag{7}$$
$$EL(\theta) = f(\theta_m, \varphi_m, \theta_{W-E}, \theta_r) \tag{8}$$

3) Formula of AZ (φ_m), EL (θ_m)

To get the AZ(φ_m) and EL(θ_m) which is the second formula, the vector $\mathbf{a_x}$, $\mathbf{a_y}$ and $\mathbf{a_z}$ must be obtained from the eqn. (5) by considering the west-east tilt. Therefore, the eqn. (5) can be rewritten as the eqn. (9).

$$X'' = A_1\mathbf{a_x} + B_1 \mathbf{a_y} + C_1\mathbf{a_z}$$
$$Y'' = A_2\mathbf{a_x} + B_2 \mathbf{a_y} + C_2\mathbf{a_z}$$
$$Z'' = A_3\mathbf{a_x} + B_3 \mathbf{a_y} + C_3\mathbf{a_z} \tag{9}$$

From the eqn. (5), we can find the vector $\mathbf{a_x}$, $\mathbf{a_y}$ and $\mathbf{a_z}$ using the inverse matrix as the eqn. (10) and eqn. (11).

$$\begin{bmatrix} \mathbf{X''} \\ \mathbf{Y''} \\ \mathbf{Z''} \end{bmatrix} = \begin{bmatrix} A_1 & B_1 & C_1 \\ A_2 & B_2 & C_2 \\ A_3 & B_3 & C_3 \end{bmatrix} \cdot \begin{bmatrix} \mathbf{a_x} \\ \mathbf{a_y} \\ \mathbf{a_z} \end{bmatrix} \tag{10}$$

$$\mathbf{a_x} = \frac{1}{D}[(B_2C_3 - B_3C_2)X'' + (B_3C_1 - B_1C_3)Y'' + (B_1C_2 - B_2C_1)Z'']$$
$$\mathbf{a_y} = \frac{1}{D}[-(A_2C_3 - A_3C_2)X'' - (A_3C_1 - A_1C_3)Y'' - (A_1C_2 - A_2C_1)X'']$$
$$\mathbf{a_z} = \frac{1}{D}[(A_2B_3 - A_3B_2)X'' + (A_3B_1 - A_1B_3)Y'' + (A_1B_2 - A_2B_1)Z''] \tag{11}$$

where

$$D = A_1(B_2C_3 - C_2B_3) + B_1(C_3C_3 - A_2C_3) + C_1(A_2B_3 - B_2A_3)$$

Substituting in the eqn. (2), the eqn. (12) is obtained by considering the definition of eqn. (1)[3].

$$\varphi_m = \tan^{-1}\left[\frac{\cos\theta \, \sin\varphi\,(B_2 C_3 - B_3 C_2) - \cos\theta \, \cos\varphi\,(A_2 C_3 - A_3 C_2)}{\cos\theta \, \sin\varphi\,(B_3 C_1 - B_1 C_3) - \cos\theta \, \cos\varphi\,(A_3 C_1 - A_1 C_3)} \right.$$

$$\left. \frac{+ \sin\theta\,(A_2 B_3 - A_3 B_2)}{+ \sin\theta\,(A_3 B_1 - A_1 B_3)}\right]$$

$$\theta_m = \sin^{-1}\left(\frac{1}{D}\{\cos\theta \, \sin\varphi(B_1 C_2 - B_2 C_1)\right.$$

$$\left. - \cos\theta \, \cos\varphi(A_1 C_2 - A_2 C_1) + \sin\theta\,(A_1 B_2 - A_2 B_1)\}\right) \qquad (12)$$

where

$$A_1 = \cos\theta_{W-E}\cos\varphi_r + \sin\theta_{W-E} \, \sin\theta_r \sin\varphi_r$$
$$B_1 = -(\cos\theta_{W-E} \, \sin\varphi_r - \sin\theta_{W-E} \, \sin\theta_r \cos\varphi_r)$$
$$C_1 = -\sin\theta_{W-E}\cos\theta_r$$
$$A_2 = \cos\theta_r \, \sin\varphi_r$$
$$B_2 = \cos\theta_r \, \cos\varphi_r$$
$$C_2 = \sin\theta_r$$
$$A_3 = \sin\theta_{W-E}\cos\varphi_r - \cos\theta_{W-E} \, \sin\theta_r \sin\varphi_r$$
$$B_3 = -(\sin\theta_{W-E}\sin\varphi_r + \cos\theta_{W-E}\sin\theta_r \cos\varphi_r)$$
$$C_3 = \cos\theta_{W-E} \, \cos\theta_r$$

4) Formula Verification Result

The verification results for these formulas are shown in the Fig. 8 and Fig. 9 although there are a little bit errors between the simulation and the measurement due to the readout drift error. The factors, φ_m and θ_m, which are input factors to eqn. (7) and eqn. (8), are the values displayed on ACU and other factors are the pre-setup values to be assumed.

Monopulse Null Point

The tracking system with five-horn has two null points of azimuth and elevation from the processing result of the comparator device. If these null points are not located at the peak line of the main beam, the shift angle from the peak line contributes to the angular error. This shift may occur due to the asymmetry of five horns during manufacturing at factory and/or the mismatch geometry among the five-horn and the main reflector and sub-reflector during installation at on site. The error of the angle shift error should be corrected after installation at on site.

In the monopulse tracking system, two identical overlapping patterns(offset $\pm\theta_S$) are formed from the equal signal axis. When the target is offset by an angle θ from this axis as the Fig. 3, the signal received through the lower pattern has greater amplitude than that received through the upper.

The field intensity at the point of antenna reception from the far field may be written as complex function of time as the eqn. (13).

$$E(t) = E_m \exp j(\omega t - \varphi_0) \qquad (13)$$

where E_m is the amplitude, ω is the angular frequency, and φ_0 is the initial phase.

The equation of gain loss for the antenna pattern is given as the equation (14)[4].

$$G(\theta) = 4 \left| \frac{J_1(\frac{\pi D}{\lambda}\sin(\theta))}{\frac{\pi D}{\lambda}\sin(\theta)} \right|^2 \tag{14}$$

where θ is offset or off-axis angle in degree, D is aperture diameter, λ is wavelength, and $J_1()$ is 1st-order Bessel function.

The normalized gain for the difference pattern is as the eqn. (15), which two squint beam patterns with the squint angle θ_S are expressed as the eqn. (16).

$$G(\theta \pm \theta_S) = k \left| \frac{J_1(u)}{u} \right|^2 \tag{15}$$

where

$$u = \frac{\pi D}{\lambda}\sin(\theta \pm \theta_S)$$

$$G_1(\theta) = kG(\theta - \theta_S), \quad G_2(\theta) = kG(\theta + \theta_S) \tag{16}$$
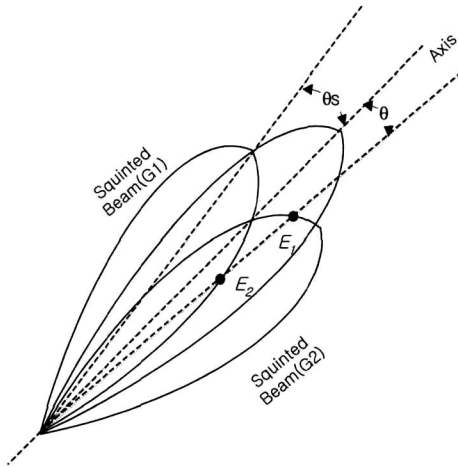

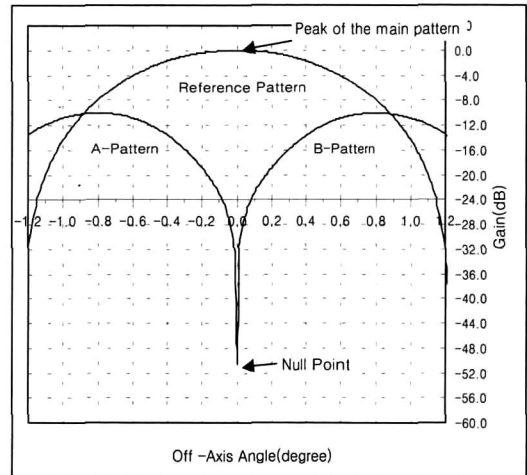Fig. 3. Reference and squint beam pattern.

Fig. 4. Reference and difference pattern of the tracking system.

The reflected signals received by two horns may be written as the real part of the complex function as the eqn. (17)[6]. In addition, the signal received by the reference pattern is given in the eqn. (18).

$$E_1(t,\theta) = E_m \cos(\omega t) * G_1(\theta), \quad E_2(t,\theta) = E_m \cos(\omega t) * G_2(\theta) \tag{17}$$

$$\sum(t,\theta) = E(t,\theta) * G(\theta) \tag{18}$$

The ratio of the received two signals which is expressed as the difference signal $\Delta(t, \theta)$ in dB beyond a hybrid of tracking systems comparator is given in the eqn. (19).

$$\Delta(t,\theta) = E_1(t,\theta,\varphi_1) - E_2(t,\theta,\varphi_2)$$
$$= E_m \cos(\omega t - \varphi_1) * G_1(\theta) - E_m \cos(\omega t - \varphi_2) * G_2(\theta) \qquad (19)$$

The phase φ_1 and φ_2, which has the phase difference of 180 degree after the comparator device, should be same or minimized because the phase difference is larger as the null depth is smaller. The Fig. 4 shows the results to be plotted from the eqn. (19) for the pattern of the TT&C antenna. Also if the null point is not the peak line of the main pattern, the monopulse slope, which determines the angle sensitivity, is shifted from center.
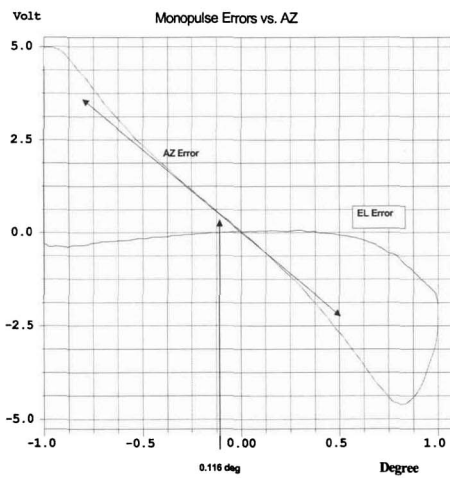

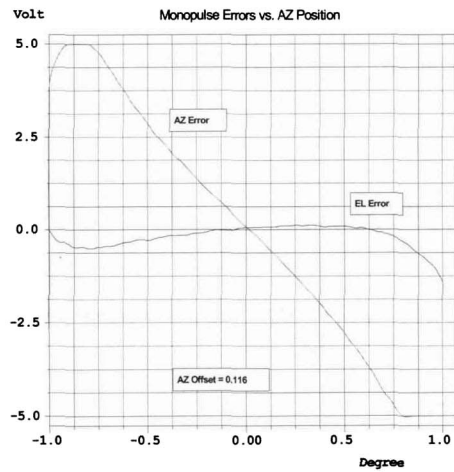**Fig. 5.** Error slope curves of the tracking system (before calibration).

Fig. 6. Error slope curves of the tracking system (after calibration).

The Fig. 5 and Fig. 6 show the error slope curve of monopulse null point alignment as the result to be processed at the monopulse processor. When the null point is shifted, the center of error slope curve is shifted.

Angular Error Verification

To verify the angular error of tracking system, one of two methods can be used. One method is to check if the azimuth and elevation angle on the ACU front panel is constant for all tilt angles from 0 to 359.999, while the monopulse tracking is performed for a fix position such as the boresight antenna or a GEO satellite. If the same angle is not displayed, the peak to peak error contributes to angular error. The other method is to do the monopulse tracking for fixed satellite or LEO satellite with a precision orbit prediction data. But this method requires the long time to find exact error value.

Before the calibration of the Tracking system, the azimuth and elevation angle were measured by using boresight for a fix position. The results were obtained as shown in the Fig. 8 and Fig. 9 with the monopulse tracking configuration as shown in the Fig. 7 and the values of the Table 1.
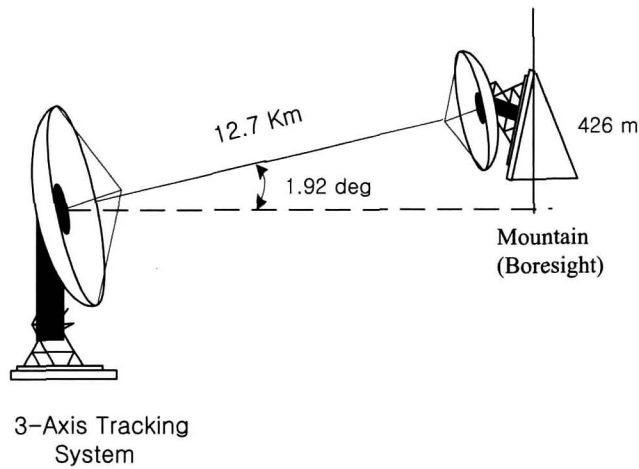
Fig. 7. AZ and EL angle measurement configuration with boresight.

From the Fig. 8 and Fig. 9, the peak to peak errors are about 0.296 deg and 0.55 deg for AZ, and EL, respectively.

Because these errors contribute to the angular error of 0.148 deg and 0.275 deg for azimuth and elevation, respectively, these errors should be corrected to the minimum value.
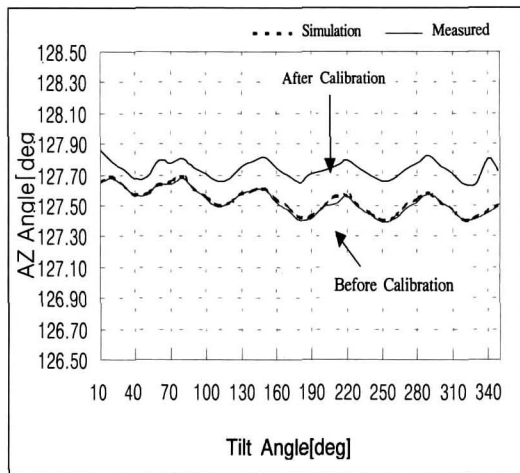

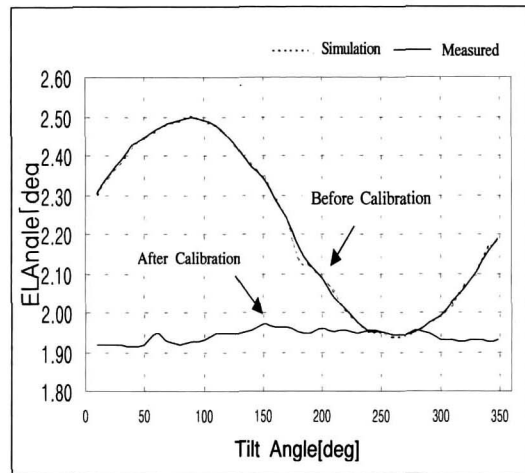**Fig. 8. Measurement and simulation of AZ before and after calibration.**

Fig. 9. Measurement and simulation of EL before and after calibration.

Simulation for Optimal Parameter

It is possible to reduce the error by the simulation with the eqn. (7) and eqn. (8). The eqn. (8) includes all factors of alignment except for scale factor (SF) and offsets factor while the eqn. (9) includes all factors of alignment except for scale factor (SF), offsets factor, and tilt angle. Because the scale factor (SF) and offsets factor are the functions of AZ/EL raw adjusted, these factors can be determined by this simulation. Although the tilt angle offset is not determined by means of the simulation, it can be determined with collection data from the location or the target of a known source.

We expect that the AZ and EL angle for all tilt angles are constant. But the peak to peaks of the results measured by the boresight before the calibrations are large as shown in the Fig. 8 and Fig. 9. It means that the combination of the factors is not optimal.

Structural Alignment Simulation

From the configuration as the Fig. 7, we can record the antenna angle ($AZ(\varphi)$, $EL(\theta)$) and the raw adjusted angle ($AZ(\varphi_m)$, $EL(\theta_m)$) on the ACU for all tilt angles while performing the monopulse tracking for each tilt position angle. The result of the antenna direction angle ($AZ(\varphi), EL(\theta)$) is presented as the Fig. 8 and Fig. 9.

Because the raw encoder data (η_{AZ}, η_{EL}) is obtained from antenna encoder without any correction on the ACU, $AZ(\varphi_m)$ and $EL(\theta_m)$ have the characteristics as the equation (20)

$$\varphi_m = \eta_{AZ} x SF_{AZ} + \delta_{AZ} \quad \text{for azimuth}$$
$$\theta_m = \eta_{EL} x SF_{EL} + \delta_{EL} \quad \text{for elevation} \tag{20}$$

where $-180^\circ < \varphi_m < 180^\circ$, η_{AZ} is AZ raw angle data, and η_{EL} is EL raw angle data.

It is possible to change the $AZ(\varphi_m)$ and $EL(\theta_m)$ by adjusting these factors which are scale factor(SF) and offset (δ). The $AZ(\varphi_m)$ and $EL(\theta_m)$ including θ_{W-E}, θ_r and φ_r are the functions of $AZ(\varphi)$ and $EL(\theta)$ as the eqn. (7) and eqn. (8). Our purpose is to seek the optimal values. That is to say, the peak to peak of the curve in the Fig. 8 and Fig. 9 are minimized by adjusting these factors. Therefore, after applying several new factors to the eqn. (7) and eqn. (8), we can find the curve with minimum error for both axes as the Fig. 8 and Fig. 9. The results of the new factors are shown in the Table 1.

In addition, it is possible to obtain the $AZ(\varphi_m)$ and $EL(\theta_m)$ angle by input the $AZ(\varphi)$ and $EL(\theta)$ angle to the eqn. (12). These are used for the verification of simulation results, which are obtained with the error pattern between the orbit prediction data and the tracking data according to the values of the scale factor (SF), offset(δ), θ_{W-E}, θ_r and φ_r.

Table 1. Alignment factor

Factor	No Calibration	Calibration
West-East tilt angle θ_{W-E}	0.0°	0.215°
North-South tilt angle θ_r	7.2°	7.0754°
AZ scale factor SF_{AZ}	1.033	1.03395
EL scale factor SF_{EL}	1.0235	1.034541
Tilt scale factor SF_{Tilt}	1.0331	1.03372
AZ offset angle δ_{AZ}	-9.036°	-9.1085°
EL offset angle δ_{EL}	9.928°	9.985°
Tilt offset angle δ_{Tilt}	1.633	1.859
Tilt angle range φ_r	10° to 348°	

Monopulse Null Point Alignment

As the eqn. (21), the null point is determined by the sequent angle θ_S. If there is the shift angle θ_{off}, it can be resolved to be given by $\theta_S \pm \theta_{off}$, where $\pm$ indicates the direction of clock-wise and counter clock-wise in case of azimuth and up and down in case of elevation.

$$G_1(\theta) = kG(\theta - \theta_S \pm \theta_{off})$$
$$G_2(\theta) = kG(\theta + \theta_S \pm \theta_{off}) \tag{21}$$

If the null point has not a shift, the amplitudes of the target signal through both patterns are equal and the difference signal will ideally have zero or the minimum magnitude as shown in the Fig. 4. However, if not, the difference signal level has not the minimum magnitude at the peak of the reference pattern. To verify the null shift error, a reference source from the far field is required such as boresight antenna. Therefore, we can find the shift angle off with spectrum analyzer. The tracking system has two RF paths of the reference and tracking chain for the monopulse tracking. The reference peak level is obtained toward the direction of the reference boresight from the reference chain. Two directions of azimuth($AZ(\varphi_1)$) and elevation($EL(\theta_1)$) are obtained. To find the difference direction, after connecting the difference chain to spectrum analyzer we can obtain the direction of azimuth($AZ(\varphi_2)$) and elevation($EL(\theta_2)$) with the minimum signal level. If there are an angle difference ($AZ(\varphi_2)-AZ(\varphi_1)$ and $EL(\theta_2)-EL(\theta_1)$) between the reference chain and difference chain, the difference is the monopulse null point error. The calibration of the monopulse null point is completed to give the shift angle to the tracking system, which has the menu for the null point shift.

The calibration of the null point was performed on-site field after installation of the tracking system and a completion of the structural alignment calibration. The error due to the null point alignment was 0.116 degree for azimuth and was free for elevation.

Results

Before the calibration, the error due to the structural alignment was ±0.148 degree for azimuth and ±0.275 degree for elevation. After the calibration, the error due to the structural alignment was reduced to ±0.075 degree for azimuth and ±0.025 degree for elevation. In addition, the error due to the monopulse null point alignment was CW 0.116 degree for elevation, which was corrected and was free for azimuth. Also, true-north direction was corrected by adjusting the tilt offset factor after collecting the result data of several satellite tracking.
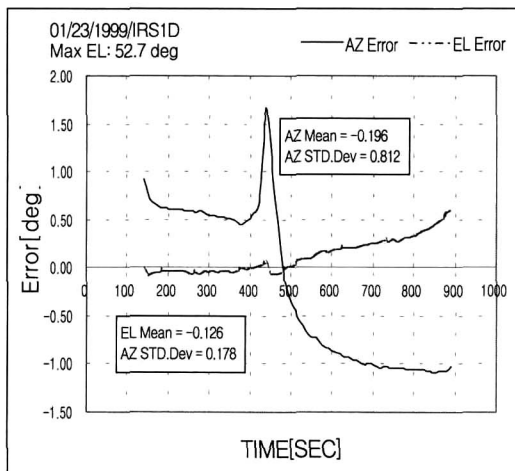

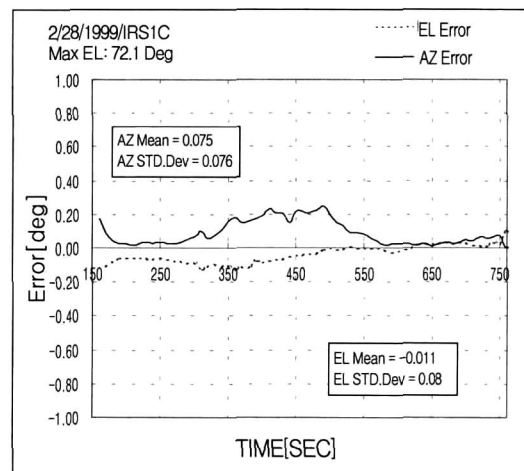**Fig. 10. Angle accuracy before calibration.**

Fig. 11. Angle accuracy after calibration.

The angle accuracy was verified with the result of the satellite tracking. During LEO satellite pass time, the tracking was performed with the program mode of predicted orbit data and the monopulse mode. The displayed angle data at ACU monitor was compared with the predicted orbit data for the accuracy calculation.

For verification of antenna alignment the satellite tracking tests were performed with IRS-ID and IRS-1C. The accuracy results are presented in the Fig. 10 and Fig. 11. Before the calibration, the angular accuracy of IRS-1D satellite was 0.831 degrees in sigma. However, the accuracy was 0.068 degrees 1 sigma after the calibration of the antenna alignment.

Conclusions

To reduce the angular error of the 3-axis tracking, the paper proposed the simulation method and the procedures to derive the formula for calibration. The formulas of the structural alignment were verified by comparing the formula result with the field measurement.

Before the calibration, the error due to the structural alignment was ± 0.148 degree for azimuth and ± 0.275 degree for elevation. After the calibration, the error due to the structural alignment was reduced to ± 0.075 degree for azimuth and ± 0.025 degree for elevation. In addition, the error due to the monopulse null point alignment was CW 0.116 degree for elevation, which was corrected and was free for azimuth. Also, true-North direction was corrected by adjusting the tilt offset factor after collecting the result data of several satellite tracking.

The antenna alignment was verified through tracking test of an operating satellite. The angle accuracy of IRS-1D was 0.831 degrees 1 sigma in stage of no calibration, but the accuracy was 0.068 degrees 1 sigma after the calibration. These error may be reduced according to the error of the predicted orbit data because these tests results were obtained under the assumption that errors of the predicted orbit data was zero.

References

[1] Krishna Kumar, Orbital and attitude prediction accuracy requirement for satellite , IEEE Transaction on Aerospace and Electronics Systems, vol. AES-17, no.1, pp.9-14, 1994

[2] Lewis V.Smith, Tracking Accuracy and Pointing Accuracy-Recommend Standard, Structures Technology for Lager Radio and Radar Telescope Systems, MIT press, 1969.

[3] Will J. Larson and James R, Werts, Space Mission Analysis and Design, Microcosm, 1992.

[4] Tri T.Ha, Digital Satellite Communications, Macmillan, Virginia Polytechnic Insatiate and Status University, 1986.

[5] Samuel M. Sherman, Monopulse Principles and Techniques, Artech House, 1984.

[6] A.I. Leonov and K.I. Fomicchev, Monopulse Radar, Artech House, 1986.